

## Volume Profile Analysis for the Reversible Binding of Superoxide to Form Iron(II)-Superoxo/Iron(III)-Peroxo Porphyrin Complexes

Katharina Dürr, Norbert Jux, Achim Zahl, Rudi van Eldik,\* and Ivana Ivanović-Burmazović\*

*Department of Chemistry and Pharmacy, University of Erlangen-Nürnberg,  
Egerlandstrasse 1, 91058 Erlangen, Germany*

Received October 15, 2010

The one-electron reduced iron(II)-dioxygen adduct,  $\{\text{Fe}^{\text{II}}-\text{O}_2\}^-$ , is known to be an important intermediate in the catalytic cycle of heme (mono)oxygenses. The same type of species, considered as  $\text{Fe}^{\text{III}}$ -peroxo, can be formed in a direct reaction between a  $\text{Fe}^{\text{II}}$  center and superoxide. In a unique high-pressure study of the reaction between superoxide and the  $\text{Fe}^{\text{II}}$  complex of a crown ether porphyrin conjugate in dimethylsulfoxide (DMSO), the overall  $\text{Fe}^{\text{II}}$ -superoxide interaction mechanism could be visualized and the nature of all species that occur along the reaction coordinate could be clarified. The equilibrium between the low-spin and high-spin forms of the starting  $\text{Fe}^{\text{II}}$  complex was quantified, which turns out to be the actual activation step toward substitution and subsequent inner-sphere electron transfer reactions. The constructed reaction volume profile demonstrates that the reaction product consists of  $\text{Fe}^{\text{III}}$ -peroxo and  $\text{Fe}^{\text{II}}$ -superoxo species that exist in equilibrium, which can better account for the versatile reactivity of  $\{\text{Fe}^{\text{II}}-\text{O}_2\}^-$  adducts toward different substrates.

### Introduction

Superoxide is the one-electron reduction product of molecular oxygen that arises during numerous oxidation reactions in both living and non-living systems. The major targets of the superoxide anion radical as reactive oxygen species under biological conditions are metal ion centers. Upon coordination to a metal ion ( $\text{M}^{n+}$ ), superoxide can be stabilized by forming metal-superoxo species ( $\text{M}^{(n+)}-\text{O}_2^-$ ) that can subsequently undergo inner-sphere electron transfer, resulting in either metal reduction and oxygen release ( $\text{M}^{(n-1)+} + \text{O}_2$ ) or formation of metal-peroxo species ( $\text{M}^{(n+1)+}-\text{O}_2^{2-}$ ).<sup>1</sup> Metal-(su)peroxo species are important intermediates in the catalytic cycles of metalloproteins, and in particular heme-proteins that are responsible for the activation of dioxygen and hydrogen peroxide, and subsequently lead to versatile oxidation processes of different substrates.<sup>2–4</sup> However, quantitative investigations of the kinetics and thermodynamics of reactions between superoxide and heme metal centers yielding metal-(su)peroxo species are almost unknown because of the instability of such product species.

By using an iron complex of a crown ether porphyrin conjugate ( $\text{H}_2\text{Porph}$ , see Chart 1 below), we were able for the first time to quantify the kinetics and thermodynamics of superoxide coordination,<sup>5</sup> and to gain more insight into the nature of the product species.<sup>6</sup> This was possible because the product of the reaction of our  $\text{Fe}^{\text{II}}$  complex with  $\text{KO}_2$  was stabilized by a positively charged moiety (crown ether chelated potassium) in close proximity to the coordinated superoxo/peroxo group. We showed in that study that  $\text{O}_2^{\bullet-}$  can react with a metal center in a reversible manner to form a quite stable iron-(su)peroxo species that can release superoxide to form the starting  $\text{Fe}^{\text{II}}$  complex by fine-tuning of the proton concentration.<sup>5</sup> Such reaction behavior is of general chemical as well as biological importance, since it shows that upon proton addition, the iron-(su)peroxo adduct does not necessarily dissociate to hydrogen peroxide and an  $\text{Fe}^{\text{III}}$  species (as in the case of SOD active enzymatic and mimetic systems)<sup>7,8</sup> or undergoes O–O bond cleavage to form a high valent oxo-iron species (as in the case of cytochrome P450). In addition, although the product of the reaction between the  $\text{Fe}^{\text{II}}$  porphyrin and superoxide was accepted to be a high-spin,

\*To whom correspondence should be addressed. E-mail: vaneldik@chemie.uni-erlangen.de (R.v.E.), ivana.ivanovic@chemie.uni-erlangen.de (I.I.-B.).

(1) Ivanović-Burmazović, I. *Adv. Inorg. Chem.* **2008**, *60*, 59–100.  
(2) Sono, M.; Roach, M. P.; Coulter, E. D.; Dawson, J. H. *Chem. Rev.* **1996**, *96*, 2841–2887.  
(3) Schlichting, I. J.; Berendzen, J.; Chu, K.; Stock, A. M.; Maves, S. A.; Benson, D. E.; Sweet, R. M.; Ringe, D.; Petsko, G. A.; Sligar, S. G. *Science* **2000**, *287*, 1615–1622.  
(4) Kim, E.; Chufan, E. E.; Kamaraj, K.; Karlin, K. D. *Chem. Rev.* **2004**, *104*, 1077–1133.

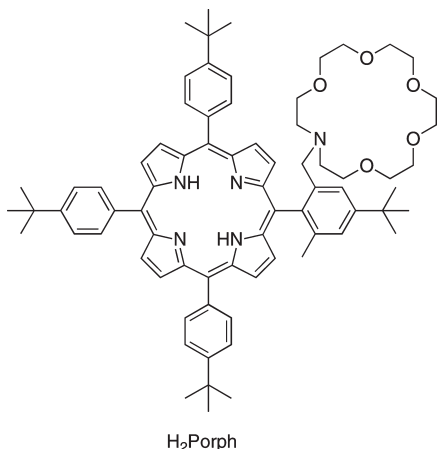
(5) Dürr, K.; Macpherson, B. P.; Warratz, R.; Hampel, F.; Tuzek, F.; Helmreich, M.; Jux, N.; Ivanović-Burmazović, I. *J. Am. Chem. Soc.* **2007**, *129*, 4217–4228.

(6) Dürr, K.; Olah, J.; Davydov, R.; Kleimann, M.; Li, J.; Lang, N.; Puchta, R.; Hübner, E.; Drewello, T.; Harvey, J. N.; Jux, N.; Ivanovic-Burmazovic, I. *J. Chem. Soc., Dalton Trans.* **2010**, *39*, 2049–2056.

(7) Batinic-Haberle, I.; Spasojevic, I.; Hambright, P.; Benov, L.; Crumbliss, A. L.; Fridovich, I. *Inorg. Chem.* **1999**, *38*, 4011–4022.

(8) Kasugai, N.; Murase, T.; Ohse, T.; Nagoka, S.; Kawakami, H.; Kubota, S. *J. Inorg. Biochem.* **2002**, *91*, 349–355.

## Chart 1



side-on Fe<sup>III</sup>-peroxo complex,<sup>9,10</sup> we recently provided evidence from spectroscopic and density functional theory (DFT) studies that in DMSO solution it coexists with its isomeric (redox-tautomer) low-spin, end-on Fe<sup>II</sup>-superoxo form.<sup>6</sup> The same species can be obtained by an one-electron reduction of a Fe<sup>II</sup>-dioxygen adduct leading to {Fe<sup>II</sup>-O<sub>2</sub>}<sup>-</sup>,<sup>11–13</sup> which is the usual pathway of its generation within catalytic cycles of the corresponding heme enzymes responsible for versatile oxidation reactions in biological systems. It seems that the real nature and reactivity of this important intermediate can be better accounted for in terms of the coexistence of two isomeric forms in equilibrium, namely, Fe<sup>II</sup>-superoxide and Fe<sup>III</sup>-peroxide.

In this work it was our goal to elucidate the mechanism of the formation of this interesting iron-(su)peroxo adduct and to obtain further information on its nature by applying high-pressure thermodynamic and kinetic techniques. Studies on the effect of pressure on forward and backward reactions, as well as on the overall reaction equilibrium, enable the construction of volume profiles that can reveal crucial mechanistic information by assisting the visualization of possible intermediates and/or transition states on the basis of partial molar volume changes that occur along the reaction coordinate.<sup>14–16</sup> Volume profiles have been extremely helpful to clarify some of the most essential mechanistic aspects and to elucidate the contribution of spin and oxidation state changes during activation processes of small molecules by metallo-enzymes and model complexes.<sup>14,16</sup> We have, therefore, performed high-pressure NMR, UV/vis, and stopped-flow measurements to be able to construct a volume profile for the reaction of our Fe<sup>II</sup> complex with superoxide. These results enlighten, for the first time in the literature, mechanistic aspects of the metal-superoxide interaction, which resulted

in the elucidation of the nature of its transition state and product species. In particular, our volume profile analysis provides evidence for the existence of an intriguing Fe<sup>II</sup>-superoxo complex in the product solution as a discrete isomer of the coexisting Fe<sup>III</sup>-peroxo complex.

## Experimental Section

**Materials.** Reagents and solvents were obtained from commercial sources (Aldrich and Acros) and were of reagent quality unless otherwise stated. DMSO was purchased as extra-dry solvent and kept under protective gas. All chemicals, except 2,4,6-tri-*t*-butylphenol (TBPh), were used as received without further purification. TBPh was recrystallized from MeOH prior to use. The synthesis of the [Fe<sup>III</sup>(Porph)Cl] complex and the preparation of the superoxide solutions have been previously reported.<sup>5</sup> The corresponding [Fe<sup>II</sup>(Porph)(DMSO)<sub>*n*</sub>] (*n* = 1, 2) complex was obtained by either chemical (with Na<sub>2</sub>S<sub>2</sub>O<sub>4</sub>) or electrochemical reduction (bulk electrolysis).

**NMR Studies.** Sample preparations were done in an Ar MBraun glovebox. Solutions of [Fe<sup>II</sup>(Porph)(DMSO)<sub>*n*</sub>] (*n* = 1, 2) were prepared by addition of an excess of Na<sub>2</sub>S<sub>2</sub>O<sub>4</sub> to a 2 mM (10 mM in case of the pressure dependent measurements) solution of [Fe<sup>III</sup>(Porph)Cl] in dry DMSO-*d*<sub>6</sub>. The suspension was stirred for 30 min. <sup>1</sup>H NMR spectra were recorded after filtration.

Temperature dependent NMR spectra in DMSO-*d*<sub>6</sub> were measured on a Bruker Avance 300 or Bruker AVANCE DRX 400WB instrument. All spectra were recorded in 5 mm outer diameter (o.d.) NMR tubes, and chemical shifts were reported as  $\delta$  (ppm) values calibrated to natural abundance deuterium solvent peaks (ppm).

A homemade high-pressure probe described in the literature was used for the variable-pressure experiments.<sup>17</sup> Pressure dependent measurements were performed in a standard 5 mm NMR tube cut to a length of 50 mm. To enable pressure transmittance to the test solution, the NMR tube was closed with a moveable KEL-S piston. The advantage of this method is that oxygen-sensitive samples can be easily placed in the NMR tube and sealed with the KEL-S piston under an argon atmosphere. A safe subsequent transfer to the high-pressure probe is assured. The pressure was applied to the high-pressure probe via a perfluorated hydrocarbon pressure medium (hexafluoropropyleneoxide, Hostinert 175, Hoechst) and measured by a VDO gauge with an accuracy of 1%. Temperature was adjusted with circulating, thermostatted water (Colora thermostat WK 16) to 0.1 K of the desired value and monitored before each measurement with an internal Pt-resistance thermometer with an accuracy of 0.2 K.<sup>18</sup> Temperature was chosen to be 320 K and kept constant, since at lower temperatures DMSO can freeze upon increasing the pressure.

**Effect of Temperature and Pressure on the Equilibrium Constant *K*<sub>1</sub>.** In analogy to Fe<sup>III</sup> porphyrins with spin admixed states,<sup>19</sup> the percentage of the low-spin species is calculated according to eq 1 ( $\delta$  is the chemical shift of the pyrrole protons of the equilibrium mixture; the limiting value for the low-spin species is about 9 ppm<sup>20</sup> and for the high-spin species about 60 ppm).<sup>21</sup>

$$\text{Int}(\%) = [(60 - \delta)/51] \times 100\% \quad (1)$$

(17) Zahl, A.; Neubrand, A.; Aygen, S.; van Eldik, R. *Rev. Sci. Instrum.* **1994**, *65*, 882.

(18) Maigut, J.; Meier, R.; Zahl, A.; van Eldik, R. *Inorg. Chem.* **2007**, *46*, 5361–5371.

(19) Ikezaki, A.; Nakamura, M. *Inorg. Chem.* **2002**, *41*, 6225–6236.

(20) (a) Shirazi, A.; Goff, H. M. *J. Am. Chem. Soc.* **1982**, *104*, 6318–6322.

(b) Walker, F. A. *The porphyrin handbook*; Academic Press: New York, 2003; Vol. 5, pp 81–182.

(21) (a) Parmely, R. C.; Goff, H. M. *J. Inorg. Biochem.* **1980**, *12*, 269–280. (b) Song, B.; Park, B.; Han, C. *Bull. Korean Chem. Soc.* **2002**, *23*, 119–122.

(9) McCandlish, E.; Miksztal, A. R.; Nappa, M.; Sprenger, A. Q.; Valentine, J. S.; Strong, J. D.; Spiro, T. G. *J. Am. Chem. Soc.* **1980**, *102*, 4268–4271.

(10) Selke, M.; Valentine, J. S. *J. Am. Chem. Soc.* **1998**, *120*, 2652–2653.

(11) Davydov, R.; Satterlee, J. D.; Fujii, H.; Sauer-Masaru, A.; Busch, D. H.; Hoffman, B. M. *J. Am. Chem. Soc.* **2003**, *125*, 16340–16346.

(12) Hersleth, H.-P.; Hsiao, Y.-W.; Ryde, U.; Goerbitz, C. H.; Andersson, K. K. *Biochem. J.* **2008**, *412*, 257–264.

(13) Unno, M.; Chen, H.; Kusama, S.; Shaik, S.; Ikeda-Saito, M. *J. Am. Chem. Soc.* **2007**, *129*, 13394–13395.

(14) Franke, A.; Hessenauer-Ilicheva, N.; Meyer, D.; Stochel, G.; Woggon, W. D.; van Eldik, R. *J. Am. Chem. Soc.* **2006**, *128*, 13611–13624.

(15) Maigut, J.; Meier, R.; Zahl, A.; van Eldik, R. *J. Am. Chem. Soc.* **2008**, *130*, 14556–14569.

(16) Hubbard, C. D.; van Eldik, R. In *Physical Inorganic Chemistry. Methods and Techniques*; Bakac, A., Ed.; Wiley: New York, 2010; pp 269–365.

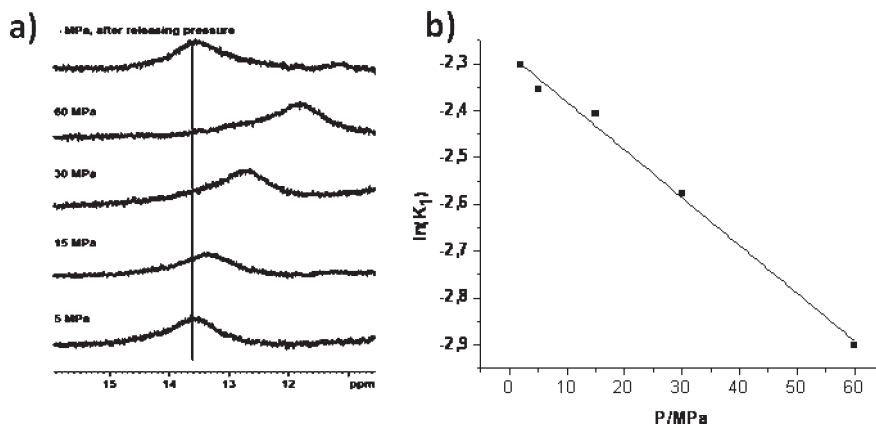


**Figure 1.** (a)  $^1\text{H}$  NMR spectrum of  $[\text{Fe}^{\text{II}}(\text{Porph})(\text{DMSO})_n]$  ( $n = 1, 2$ ) at 320 K and different pressures; (b) plot of  $\ln(K_1)$  versus pressure. The pressure range was limited to 60 MPa because of the interference of the paramagnetic signal at higher pressures with a signal of the high pressure medium.

The species distribution at different temperatures and pressures is summarized in Supporting Information, Table S1. From these results the equilibrium constant  $K_1$  (in which the activity of solvent is considered to be 1) can be calculated according to eq 2. On the basis of the temperature and pressure dependent data for  $K_1$  the corresponding thermodynamic parameters can be estimated according to eqs 3 and 4, respectively.<sup>22</sup>

$$K_1 = [\text{HS}]/[\text{LS}] \quad (2)$$

where [HS] is the high-spin *mono*-DMSO complex concentration, and [LS] is the low-spin *bis*-DMSO complex concentration

$$\ln(K_1) = -\Delta H^\circ/RT + \Delta S^\circ/R \quad (3)$$

$$[\partial \ln(K_1)/\partial P]_T = -\Delta V^\circ/RT \quad (4)$$

The reaction enthalpy  $\Delta H^\circ$  was obtained from the slope and the reaction entropy  $\Delta S^\circ$  from the intercept of the plot of  $\ln(K_1)$  versus  $1/T$  (see Supporting Information, Figure S3). The reaction volume  $\Delta V^\circ$  results from the slope of the plot of  $\ln(K_1)$  versus pressure (see Figure 1).

**High Pressure UV/vis Measurements.** Sample preparation was done in an Ar MBraun glovebox. A sample of  $\text{K}[\text{Fe}^{\text{III}}(\text{Porph})(\text{O}_2^{2-})]$  was prepared by addition of an excess of  $\text{KO}_2$  to a  $10^{-5}$  M solution of  $[\text{Fe}^{\text{III}}(\text{Porph})\text{Cl}]$  in a dry DMSO solution of 0.1 M  $(n\text{-Bu})_4\text{NPF}_6$  (tetrabutylammonium hexafluorophosphate). The suspension was stirred for 30 min. High pressure UV/vis spectra were recorded after filtration.

Spectral measurements at elevated pressure were performed in a pill-box cuvette on a Shimadzu UV-2101-PC spectrophotometer using a homemade high-pressure cell.<sup>23</sup> The high-pressure pump was purchased from NOVA SWISS (Nova Werke AG, CH-8307 Effretikon, Vogelsangstrasse); it allows measurements up to 150 MPa.

**High Pressure Stopped-Flow Kinetics and Data Processing.** The preparation of  $\text{KO}_2$  solutions in DMSO and determination of superoxide concentrations have previously been reported.<sup>5</sup> The presence of  $(n\text{-Bu})_4\text{NPF}_6$ , which was used to provide the constant ionic strength (0.1 M) in the kinetic measurements, in general increases the superoxide solution stability.

Solutions of  $[\text{Fe}^{\text{II}}(\text{Porph})(\text{DMSO})_n]$  ( $n = 1, 2$ ) were prepared by bulk electrolysis of  $10^{-5}$  M solutions of the respective iron(III) porphyrin in DMSO at  $-0.2$  V versus Ag/AgCl. 0.1 M of  $\text{Bu}_4\text{NPF}_6$  was also present in solution as electrolyte. During

the electrolysis the time-resolved UV/vis spectra were recorded simultaneously in situ. Electrochemical reduction was performed under nitrogen at a Pt gauze working electrode with an Ag wire pseudo reference electrode and a platinated Ti auxiliary electrode separated from the working electrode compartment by a glass frit. Potential or current were controlled with an Autolab instrument with PGSTAT 30 potentiostat. The experiment was stopped when no change in the UV/vis spectra was observed anymore. Time-resolved UV/vis spectra were recorded by use of a Hellma 661.502-QX quartz Suprasil immersion probe attached via optical cables to a 150 W Xe lamp and a multiwavelength J & M detector.

A solution of  $\text{K}[\text{Fe}^{\text{III}}(\text{Porph})(\text{O}_2^{2-})]$  to monitor the “off” reaction was prepared as described above for the high pressure UV/vis measurements.

All kinetic measurements were carried out under pseudo-first-order conditions at a complex concentration of  $5 \times 10^{-6}$  M and superoxide concentration of  $10^{-4}$  M. The superoxide concentration was selected on the basis of earlier concentration dependent measurements, which resulted in a linear dependence of  $k_{\text{obs}}$  on the superoxide concentration, with a negligible intercept, for the “on” reaction.<sup>5</sup> Measurements under high pressure were carried out using a homemade high-pressure stopped-flow instrument,<sup>24</sup> for which Isolast O-rings were also used for all syringe seals. The stopped-flow instrument was thermostatted at 35 °C. The reactions were monitored at 440 and 430 nm, which correspond to the absorption maxima of the product and reactant complex, respectively (see Figures 9 and 11 in reference 5). Values of  $\Delta V^\ddagger$  were calculated from the slope of plots of  $\ln(k)$  versus pressure (Supporting Information, Figures S4 and S5) in the usual manner based on eq 5. For monitoring the “on” reaction, DMSO solutions of  $[\text{Fe}^{\text{II}}(\text{Porph})(\text{DMSO})_n]$  ( $n = 1, 2$ ) and  $\text{KO}_2$  were mixed in the high pressure stopped-flow. For the measurement of  $k_{\text{obs}}$  for the “on” reaction as a function of pressure, fresh solutions of superoxide and the reactant complex were prepared under ambient conditions and thermostatted for 20 min at elevated pressure in the stopped-flow, before mixing them to measure  $k_{\text{obs}}$  (Supporting Information, Table S2). For monitoring the “off” reaction at each pressure, fresh solutions of  $\text{K}[\text{Fe}^{\text{III}}(\text{Porph})(\text{O}_2^{2-})]$  and a moderate acid, TBPh, were prepared and thermostatted for 20 min at elevated pressure in the stopped-flow, before mixing them to determine  $k_{\text{obs}}$  (Supporting Information, Table S3).

$$[\partial \ln(k)/\partial P]_T = -\Delta V^\ddagger/RT \quad (5)$$

Determination of  $k_{\text{obs}}$  for the “on” reaction, which depends linearly on  $[\text{O}_2^-]$ ,<sup>5</sup> is complicated by the fact that superoxide

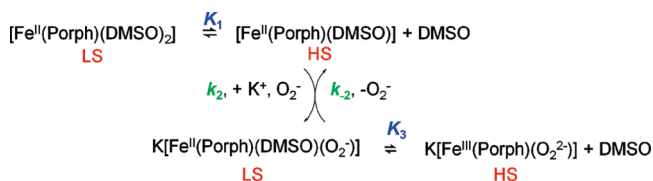
(22) Wilkins, R. G. *Kinetics and Mechanisms of Reactions of Transition Metal Complexes*; VCH: New York, 1991.

(23) (a) Spitzer, M.; Gartig, F.; van Eldik, R. *Rev. Sci. Instrum.* **1988**, *59*, 2092–2093. (b) Fleischmann, K. F.; Conze, G. E.; Stranks, R. D.; Kelm, H. *Rev. Sci. Instrum.* **1974**, *45*, 1427.

(24) (a) van Eldik, R.; Palmer, D. A.; Schmidt, R.; Kelm, H. *Inorg. Chim. Acta* **1981**, *50*, 131–135. (b) van Eldik, R.; Gaede, W.; Wieland, S.; Kraft, J.; Spitzer, M.; Palmer, D. A. *Rev. Sci. Instrum.* **1993**, *64*, 1355–1357.



**Scheme 1.** Reaction Scheme Summarizing the Existing Equilibria and Superoxide Reaction with the Fe<sup>II</sup> Porphyrin in DMSO<sup>a</sup>



<sup>a</sup>The reactant exists in a spin state equilibrium  $K_1$  (here: low-spin = LS,  $S = 0$ ; high-spin = HS,  $S = 2$ ). The reaction of  $\text{KO}_2$  with this equilibrium mixture and the dissociation of (super)oxide are characterized by the rate constants  $k_2$  and  $k_{-2}$ , respectively. The product complex exists in a spin/redox state equilibrium  $K_3$  (here:  $\text{Fe}^{\text{II}}$  low-spin = LS,  $S = 0$ ;  $\text{Fe}^{\text{III}}$  high-spin = HS,  $S = 5/2$ ).

undergoes disproportionation, that is, spontaneous decomposition, during the time required to thermostat the solutions at elevated pressure. The disproportionation of superoxide is a second order process and expected to be accelerated by increasing pressure. As a consequence, the superoxide concentration after thermostating the solutions at elevated pressure, before mixing them to determine  $k_{\text{obs}}$ , will be somewhat lower than prepared at ambient pressure, which will lower the apparent  $k_{\text{obs}}$  value. Therefore, the apparent activation volume needs to be corrected for this effect according to eq 6 to obtain the actual  $\Delta V^\ddagger(k_{\text{obs}})$  value for the “on” reaction.

$$\Delta V^\ddagger_{(app)} = \Delta V^\ddagger(k_{obs}) + \Delta V^\ddagger_{(corr)} \quad (6)$$

To determine the value of  $\Delta V^{\ddagger}_{(corr)}$  we measured the time dependence of  $k_{obs}$  at three different pressures (Supporting Information, Table S4).

The slopes obtained from the linear time dependence of  $\ln(k_{\text{obs}})$  (Supporting Information, Figure S6) were plotted versus pressure (Supporting Information, Figure S7, Table S5), and from the corresponding slope,  $[\partial \ln(k_{\text{obs}})/\partial t]/\partial P = -(1.07 \pm 0.06) \times 10^{-4} \text{ cm}^3 \text{ J}^{-1} \text{ min}^{-1}$ ,  $\Delta V^\ddagger_{(\text{corr})}$  was obtained according to eq 7 (for the calculation see Supporting Information).

$$\Delta V^{\ddagger}_{(corr)} = -[\partial \ln(k_{obs})/\partial t)]/\partial P \times \partial t \times RT \quad (7)$$

## Results and Discussion

**Pressure and Temperature Dependent NMR Study of the Complex  $[\text{Fe}^{\text{II}}(\text{Porph})(\text{DMSO})_n]$  ( $n = 1, 2$ ).** Solvation of iron(II) tetraphenylporphyrins in DMSO leads to an equilibrium between five- and six-coordinate species with one or two coordinated DMSO molecules, respectively.<sup>5,20,21</sup> Since such an equilibrium ( $K_1$  in Scheme 1) also exists in solution for the reactant complex,  $[\text{Fe}^{\text{II}}(\text{Porph})(\text{DMSO})_n]$  ( $n = 1, 2$ ), we performed temperature and pressure dependent  $^1\text{H}$  NMR measurements to study the thermodynamics of the underlying equilibrium process.

Literature data on NMR spectra of  $[\text{Fe}^{\text{II}}(\text{TPP})]$  (TPP = dianion of tetraphenylporphrin) in DMSO show that the complex exists in a mixture of low-spin and high-spin species,<sup>20,21</sup> with a moderately broad paramagnetic signal of the pyrrole protons around 12 ppm for the high-spin species. This finding corresponds directly to the  $^1\text{H}$  NMR spectrum of the investigated  $[\text{Fe}^{\text{II}}(\text{Porph})(\text{DMSO})_n]$  ( $n = 1, 2$ ) system (see Supporting Information, Figure S1).

In the range from 0 to 10 ppm, there are signals with only minor line broadening that correspond to the signals of the diamagnetic  $[\text{Fe}^{\text{II}}(\text{Porph})(\text{DMSO})_2]$  species. The

**Table 1.** Thermodynamic Parameters for the Equilibrium Constant  $K_1$

$K_1$ at 298.2 K	$0.030 \pm 0.001$
$\Delta H^\circ/\text{kJ mol}^{-1}$	$+48 \pm 1$
$\Delta S^\circ/\text{J K}^{-1} \text{mol}^{-1}$	$+133 \pm 3$
$\Delta G^\circ/\text{kJ mol}^{-1}$ at 298.2 K	$+9 \pm 2$
$\Delta V^\circ/\text{cm}^3 \text{mol}^{-1}$ at 320 K	$+26 \pm 2$

broad signal around 11 ppm (see Supporting Information, Figure S1) belongs to the resonance of the pyrrole protons of the paramagnetic  $[\text{Fe}^{\text{II}}(\text{Porph})(\text{DMSO})]$  species. The position and line broadening of the pyrrole protons of a porphyrin system are generally used to determine the spin state of the central metal.<sup>20b</sup> The remaining paramagnetic resonances of  $[\text{Fe}^{\text{II}}(\text{porphyrin})-(\text{DMSO})]$  cannot be observed, as they are merged with the diamagnetic ones.

On increasing the temperature the paramagnetic signal shifts strongly to lower field (see Supporting Information, Figure S2), whereas the rest of the spectrum remains almost unchanged. The line broadening increases only moderately. The reason for this behavior is a shift of  $K_1$  in Scheme 1 in favor of the paramagnetic  $[\text{Fe}^{\text{II}}(\text{Porph})\text{-(DMSO)}]$  complex. After allowing the sample to cool down, the starting spectrum is regained as the equilibrium is restored. This demonstrates the existence of a reversible low-spin/high-spin equilibrium, where the contribution of the high-spin species increases with increasing temperature.

Since the low-spin/high-spin equilibrium constant  $K_1$  should also be pressure sensitive, we performed pressure dependent  $^1\text{H}$  NMR measurements (Figure 1). Increasing pressure results in a shift of the equilibrium to the diamagnetic low-spin species. This is expected as pressure favors DMSO coordination and the formation of the low-spin species. On decreasing pressure the larger contribution of the high-spin species (Figure 1a) is restored as in the starting state of the equilibrium.

The temperature and pressure dependent measurements enable the quantification of the thermodynamic parameters for the equilibrium  $K_1$  in Figure 1, which are summarized in Table 1 (for details see Experimental Section and Supporting Information, Table S1).

The temperature dependence plot of  $\ln(K_1)$  (see Supporting Information, Figure S3) was found to be linear and resulted in significantly positive values for the thermodynamic parameters  $\Delta H^\circ$  and  $\Delta S^\circ$  (Table 1). They are in agreement with the endothermic and dissociative character of the underlying low-spin to high-spin transition. The values of  $K_1$  and corresponding species distribution (see Supporting Information, Table S1) show that in DMSO solution mostly the low-spin *bis*-DMSO complex exists (97% at 298 K and 0.1 MPa). The pressure dependence of  $\ln(K_1)$  also gave a straight line (Figure 1b) and resulted in  $\Delta V^\circ = +26 \pm 2 \text{ cm}^3 \text{ mol}^{-1}$ . The high positive reaction volume is a result of DMSO dissociation that accompanies the spin-state change on the Fe center. It is known that the low-spin/high-spin transformation in iron model complexes and enzymatic (cytochrome P450) systems is accompanied by a volume increase of between 12 and 15  $\text{cm}^3 \text{ mol}^{-1}$ ,<sup>14</sup> suggesting that the additional volume expansion of 11–14  $\text{cm}^3 \text{ mol}^{-1}$  found in the present case can be ascribed to the dissociation of DMSO. From a comparison with other similar processes on iron systems,<sup>14</sup> it seems that the volume change of  $\sim 30 \text{ cm}^3 \text{ mol}^{-1}$  is in

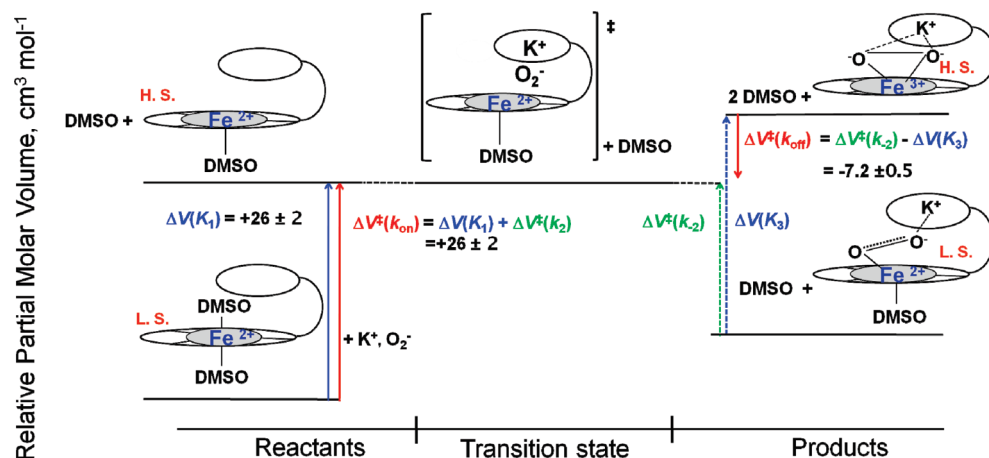


**Figure 2.** Volume profile for the reversible binding of superoxide to the Fe(II) porphyrin. (All depicted volume changes along the reaction coordinate are given in  $\text{cm}^3 \text{mol}^{-1}$  and discussed in the manuscript.)

general characteristic for the change in coordination number on the iron center coupled to a spin-state transformation.

**Pressure Dependence of the Reversible Reaction with Superoxide.** Since we have now quantified the effect of pressure on the equilibrium between the two  $[\text{Fe}^{\text{II}}(\text{Porph})(\text{DMSO})_n]$  ( $n = 1, 2$ ) species in DMSO solution (vide supra), we further performed high-pressure stopped-flow studies on the reaction of these complexes with  $\text{KO}_2$ . We have previously shown that this is a reversible reaction (Scheme 1) and have quantified the corresponding overall superoxide binding constant ( $K$ ), both thermodynamically (UV–vis titration) and kinetically (by determining the  $k_{\text{on}}$  and  $k_{\text{off}}$  rate constants,  $K = k_{\text{on}}/k_{\text{off}}$ , vide infra), as well as the activation parameters ( $\Delta H^\ddagger$  and  $\Delta S^\ddagger$ ) for the forward, “on”, reaction.<sup>5</sup>

By following the coordination of superoxide to the iron(II) complex by high-pressure UV–vis stopped-flow technique, we obtained the pressure dependence of  $k_{\text{on}}$ . From the linear pressure dependence of  $\ln(k_{\text{obs}})$  for the “on” reaction (see Supporting Information, Figure S4) and eq 5 the apparent activation volume was found to be  $+32 \pm 2 \text{ cm}^3 \text{mol}^{-1}$ . Since the spontaneous decomposition of superoxide is a second order reaction, it is somewhat accelerated with pressure and results in an intrinsically lower superoxide concentration present in solution at elevated pressures. This leads to an additional decrease of the  $k_{\text{obs}}$  values for the “on” reaction ( $k_{\text{obs}}$  depends linearly on  $[\text{O}_2^-]$ )<sup>5</sup> with increasing pressure and positive volume contribution ( $+5.5 \pm 0.3 \text{ cm}^3 \text{mol}^{-1}$ , see Experimental Section and Supporting Information). Thus, after correction for this effect the actual activation volume for the “on” reaction was found to be  $\Delta V^\ddagger(k_{\text{on}}) = (+32 - (+6)) \pm 2 = +26 \pm 2 \text{ cm}^3/\text{mol}$ .

The backward “off” reaction can be followed by addition of a controlled concentration of a proton source to the product mixture, to decompose the excess of superoxide present in solution ( $2\text{O}_2^- + 2\text{H}^+ \rightarrow \text{O}_2 + \text{H}_2\text{O}_2$ ) and to shift the reaction equilibrium back to the starting iron(II) species (Scheme 1).<sup>5</sup> 2,4,6-tri-*(t*-butyl)phenol, TBPh, was used as a moderate acid. We have previously shown that the rate of the “off” reaction (release of superoxide) does not depend on [TBPh] which behaves as a trapping agent.<sup>5</sup> By following the formation of iron(II) species upon mixing the reaction product with a solution

of 2,4,6-tri-*(t*-butyl)phenol in the high-pressure stopped-flow, the activation volume for the “off” reaction could be obtained, namely,  $\Delta V^\ddagger(k_{\text{off}}) = -7.2 \pm 0.5 \text{ cm}^3 \text{mol}^{-1}$ , from the slope of the linear dependence of  $\ln(k_{\text{off}})$  on pressure (see Supporting Information, Figure S5).

**Volume Profile Analysis for the Reversible Binding of Superoxide.** On the basis of the above presented results, the volume profile for the overall reaction can be depicted as in Figure 2.

As a result of the fact that the overall reaction mechanism involves a pre-equilibrium between low-spin and high-spin  $[\text{Fe}^{\text{II}}(\text{Porph})(\text{DMSO})_n]$  ( $n = 1, 2$ ) species, the observed rate constant for the reaction with superoxide can be expressed by eq 8, where  $k_2$  is the forward rate constant for the coordination of  $\text{O}_2^-$ ,  $K_1$  is the pre-equilibrium constant, and  $k_{\text{off}} = k_{-2}/(1 + K_3)$  is the overall reverse rate constant (Scheme 1).

$$k_{\text{obs}} = \{K_1 k_2 [\text{O}_2^-] / (1 + K_1)\} + k_{-2} / (1 + K_3) \quad (8)$$

Equation 8 can be simplified to  $k_{\text{obs}} = K_1 k_2 [\text{O}_2^-] + k_{-2}/K_3$  since  $K_1$  is 0.03 M at 298.2 K, that is,  $K_1 \ll 1$  (see Table 1), and spectroscopic observations showed that the reaction product predominantly exists in the peroxo form,<sup>5,6,9,10</sup> that is,  $K_3 \gg 1$ . It follows that  $k_{\text{obs}} = k_{\text{on}}[\text{O}_2^-] + k_{\text{off}}$ , with the second-order rate constant for superoxide binding  $k_{\text{on}} = K_1 k_2$  and first-order rate constant for superoxide release  $k_{\text{off}} = k_{-2}/K_3$ . Thus, the obtained activation volume for the “on” reaction,  $\Delta V^\ddagger(k_{\text{on}})$ , involves contributions from the effect of pressure on the equilibrium between six- and five-coordinate iron(II) species,  $\Delta V^\circ(K_1)$ , and on the rate constant for the binding of superoxide  $k_2$ ,  $\Delta V^\ddagger(k_2)$  (see Scheme 1 and Figure 2). Interestingly, the experimental values of  $\Delta V^\circ(K_1)$  and  $\Delta V^\ddagger(k_{\text{on}})$  are identical and consequently it follows that  $k_2$  for the rate-determining step must be almost pressure-independent, that is,  $\Delta V^\ddagger(k_2) \sim 0 \text{ cm}^3 \text{mol}^{-1}$ . This allows us to visualize the transition state for the binding of superoxide as “early” and reactant-like in terms of volume changes, that is, it has the nature of the five-coordinate mono-DMSO high-spin  $[\text{Fe}^{\text{II}}(\text{Porph})(\text{DMSO})]$  complex. We have previously reported  $\Delta H^\ddagger(k_{\text{on}}) = 61.2 \pm 0.9 \text{ kJ mol}^{-1}$  and  $\Delta S^\ddagger(k_{\text{on}}) = +48 \pm 3 \text{ J K}^{-1} \text{mol}^{-1}$  for the overall binding process,<sup>5</sup> and based on the herein determined

$\Delta H^\circ(K_1)$  and  $\Delta S^\circ(K_1)$  values (Table 1) it follows that  $\Delta H^\ddagger(k_2) = \Delta H^\ddagger(k_{\text{on}}) - \Delta H^\circ(K_1) = 13 \text{ kJ mol}^{-1}$  and  $\Delta S^\ddagger(k_2) = \Delta S^\ddagger(k_{\text{on}}) - \Delta S^\circ(K_1) = -85 \text{ J K}^{-1} \text{ mol}^{-1}$ . These parameters further clarify the nature of the transition state and activation process. The low value of  $\Delta H^\ddagger(k_2)$  confirms the existence of the “early” transition state. The significantly negative  $\Delta S^\ddagger(k_2)$  can be accounted for in terms of chelation of the weakly solvated  $\text{K}^+$  in DMSO by the dangling crown ether and the entrance of  $\text{O}_2^-$  into the pocket between the porphyrin and the crown ether moiety (Figure 2). The volume neutrality of the activation process is a result of the opposite effects of the intrinsic volume decrease caused by chelation of  $\text{K}^+$  and uptake of free  $\text{O}_2^-$  within the coordination pocket, and the volume increase caused by the desolvation of free  $\text{K}^+$  and  $\text{O}_2^-$  on entering the crown ether and coordination pocket, respectively.

Along the reaction coordinate between an  $\text{Fe}^{\text{II}}$  species and  $\text{KO}_2$  it is expected that the iron(II)-superoxo complex appears either as a transition state, intermediate, or as a product species. The value of the activation volume for the “off” reaction, namely,  $\Delta V^\ddagger(k_{\text{off}}) = -7.2 \pm 0.5 \text{ cm}^3 \text{ mol}^{-1}$ , offers valuable information to elucidate the role of this species in the overall reaction mechanism. Our previous studies have shown that such a species in DMSO exists as the six-coordinate, low-spin  $\text{K}[\text{Fe}^{\text{II}}(\text{Porph})(\text{DMSO})(\text{O}_2^-)]$  complex,<sup>6</sup> requiring a large negative value for  $\Delta V^\ddagger(k_2)$  of approximate  $-26 \text{ cm}^3 \text{ mol}^{-1}$  (which is clearly not the case, vide supra) if it would act as the transition state. On the basis of the principle of microscopic reversibility, the reaction must pass through the same transition state in the rate-determining step, approaching it from either the forward or the reverse direction. Therefore, if the iron(II)-superoxo species would exist as an intermediate between the  $\text{Fe}^{\text{II}}$  and  $\text{Fe}^{\text{III}}$ -peroxo complexes, the activation process in the back direction would involve transformation from this low-spin, six-coordinate  $\text{Fe}^{\text{II}}\text{--O}_2^-$  intermediate to the high-spin, five-coordinate transition state (vide supra). This process would require a quite positive  $\Delta V^\ddagger(k_{\text{off}})$ , which would correspond to  $\Delta V^\ddagger(k_{-2})$  depicted in Figure 2. The experimentally obtained moderately negative value of  $\Delta V^\ddagger(k_{\text{off}})$  can only be accounted for if the involvement of an equilibrium between the low-spin  $\text{Fe}^{\text{II}}$ -superoxo and high-spin  $\text{Fe}^{\text{III}}$ -peroxo species in the product solution is taken into consideration. This supports our suggestion that the high-spin  $\text{Fe}^{\text{III}}$ -peroxo complex must coexist in equilibrium with its redox-tautomer, low-spin  $\text{Fe}^{\text{II}}$ -superoxo form, and therefore  $\Delta V^\ddagger(k_{\text{off}})$  is the sum of two contributions, namely,  $\Delta V^\ddagger(k_{\text{off}}) = \Delta V^\ddagger(k_{-2}) - \Delta V^\circ(K_3)$  since  $k_{\text{off}} = k_{-2}/K_3$  (see Scheme 1 and Figure 2). The value of  $\Delta V^\circ(K_3)$  is expected to be very similar to that of  $\Delta V^\circ(K_1)$  because of the similarity of the overall reactions involved, that is, about  $+26 \text{ cm}^3 \text{ mol}^{-1}$ , which leads to the overall negative value found for  $\Delta V^\ddagger(k_{\text{off}})$ , namely,  $-7.2 \pm 0.5 \text{ cm}^3 \text{ mol}^{-1}$ .

Further confirmation for the existence of the high-spin/low-spin equilibrium in the product state was obtained by monitoring the UV–vis spectrum of the product solution as a function of pressure. As expected the increasing pressure causes a small but significant red-shift of the Soret absorption band (see Figure 3), indicating a shift of the equilibrium toward the low-spin

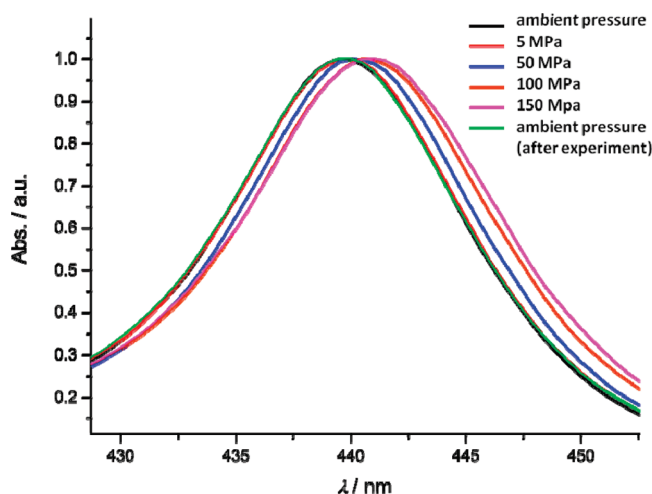


**Figure 3.** Pressure dependent UV/vis spectra of the iron(su)peroxo product complex. UV/vis spectra of the reaction product ( $10^{-5} \text{ M}$ ) as a function of pressure at  $35^\circ\text{C}$  in the presence of  $0.1 \text{ M}$   $(n\text{-Bu})_4\text{NPF}_6$  were obtained by use of a pill-box cuvette combined with a high-pressure optical cell (see Experimental Section).

six-coordinate component of the product mixture. This is in agreement with what has been observed on studying temperature dependent spectra of liver microsomal cytochrome P450 in the presence of different substrates.<sup>25</sup> On releasing pressure the starting spectrum was obtained, which demonstrates the reversibility of the pressure induced change in the equilibrium position. The quantification of the equilibrium constant  $K_3$  could not be achieved since the spectra of the pure iron(II)-superoxo or pure iron(III)-peroxo form are yet unknown, and there is no corresponding data available in the literature. Therefore, future studies will be required to tune this equilibrium such that it can be pushed completely in either the one or the other direction to independently characterize these two species.

## Conclusions

In this paper, for the first time, the thermodynamics of the iron(II) porphyrin low-spin/high-spin equilibrium and high-pressure studies on the reversible binding of superoxide to a metal center are reported. The obtained results elucidate the overall metal-superoxide reaction mechanism and the nature of all species that appear along the reaction coordinate. On the basis of the overall volume profile presented in Figure 2, the nature of the transition state is almost identical to that of the high-spin five-coordinate complex in the reactant state showing that the spin change on the iron(II) porphyrin center is crucial for its reactivity and activates it toward substitution and consequently inner-sphere electron transfer processes. The only difference between the high-spin complex of the reactant state and the transition state is that the latter contains  $\text{KO}_2$  in the pocket between the porphyrin and the covalently attached crown ether moiety so that the superoxide is in a close proximity to the reactive iron center. The volume profile reveals that the product solution contains an equilibrium mixture of the high-spin iron(III)-peroxo and low-spin iron(II)-superoxo complexes. The pressure dependence of the UV/vis spectrum of the product solution confirms the presence of this equilibrium. These results offer strong support

(25) Rein, H.; Ristau, O.; Friedrich, J.; Jänig, G.-R.; Ruckpaul, K. *FEBS Lett.* **1977**, *75*, 19–22.

for the existence of the iron(II)-superoxo species not as a resonance form of the iron(III)-peroxo but as a discrete stable complex in solution, which is in perfect agreement with our recent report on the corresponding Mössbauer-, EPR-, and mass-spectra of the reaction product, as well as DFT calculations.<sup>6</sup>

The existence of two different forms of Fe<sup>II</sup>-superoxide adducts, that is, the reduced Fe<sup>II</sup>-dioxygen adduct, is very intriguing because it can better account for their versatile reactivity toward different substrates.<sup>26</sup> In general, superoxo species are prone to abstract a hydrogen atom,<sup>27</sup> whereas peroxo species exhibit rather nucleophilic reactivity.<sup>10,28</sup> Thus, future work should be directed toward understanding

the effects of the solvent, a *trans* ligand, and possible involvement of coordinated peroxide/superoxide in hydrogen bonding or electrostatic interactions, on the structure and electronic properties of the heme iron-superoxide adducts and the peroxo/superoxo equilibrium, as well as their reactivity toward different organic substrates of biological and synthetic interest. To reveal the effect of the nearby positive charge, we are currently studying the analogous iron porphyrin complex without covalently attached crown ether.

**Acknowledgment.** This work was supported by the Deutsche Forschungsgemeinschaft through SFB 583 "Redox-active metal complexes".

**Supporting Information Available:** Temperature dependent NMR spectra of [Fe<sup>II</sup>(Porph)(DMSO)<sub>n</sub>] (*n* = 1, 2), species distribution and the values of *K*<sub>1</sub> at different temperatures and pressures, plot of ln(*K*<sub>1</sub>) versus 1/*T*, pressure dependent rate constants for the "on" and "off" reaction, pressure dependence of ∂ ln(*k*<sub>obs</sub>)/∂*t* for the "on" reaction. This material is available free of charge via the Internet at <http://pubs.acs.org>.

(26) Selke, M.; Sisemore, M. F.; Valentine, J. S. *J. Am. Chem. Soc.* **1996**, *118*, 2008–2012.

(27) (a) Bollinger, J. M.; Krebs, C. *Curr. Opin. Chem. Biol.* **2007**, *11*, 151–158. (b) Mukherjee, A.; Cranswick, M. A.; Chakrabarti, M.; Paine, T. K.; Fujisawa, K.; Münck, E.; Que, L., Jr. *Inorg. Chem.* **2010**, *49*, 3618–3628.

(28) (a) Park, M. J.; Lee, J.; Suh, Y.; Kim, J.; Nam, W. *J. Am. Chem. Soc.* **2006**, *128*, 2630–2634. (b) Seo, M. S.; Kim, J. Y.; Annaraj, J.; Kim, Y.; Lee, Y.-M.; Kim, S.-J.; Kim, J.; Nam, W. *Angew. Chem., Int. Ed.* **2007**, *46*, 377–380.